*International Journal of Minerals, Metallurgy and Materials*
*Volume 17, Number 1, February 2010, Page 46*
**DOI: 10.1007/s12613-010-0108-z**

# Deformation behavior and microstructure of an Al-Zn-Mg-Cu-Zr alloy during hot deformation

*Liang-ming Yan, Jian Shen, Jun-peng Li, Zhou-bing Li, and Xiao-dong Yan*

General Research Institute for Nonferrous Metals, Beijing 100088, China
(Received: 26 February 2009; revised: 23 March 2009; accepted: 3 April 2009)

**Abstract:** The hot deformation behavior and microstructures of Al-7055 commercial alloy were investigated by axisymmetric hot compression at temperatures ranging from 300°C to 450°C and strain rates from $10^{-2}$ to 10 $s^{-1}$, respectively. Microstructures of deformed 7055 alloy were investigated by transmission electron microscopy (TEM). The dependence of peak stress on deformation temperature and strain rate can be expressed by the hyperbolic-sine type equation. The hot deformation activation energy of the alloy is 146 kJ/mol. Moreover, the flow stress curves predicted by the modified constitutive equations are reasonably consistent with the experimental results, which confirms that the proposed deformation constitutive equations can provide evidence for the selection of hot forming parameters. TEM results indicate that dynamic recovery is the main softening mechanism during hot deformation.

**Keywords:** aluminum alloys; dynamic recovery; hot compression; deformation behavior; constitutive equation

## 1. Introduction

The aerospace industry has a great interest in developing new high strength aluminum alloys. Aluminum alloy 7055 is a major candidate for such applications, which is mainly produced in the form of both plates and extrusions [1-3]. So far, 7055-T77 aluminum alloy has attracted more and more attention for the excellent combination properties of high strength, high fracture toughness, low density, and good corrosion resistance [4]. The microstructures after heat treatment, such as second phases and precipitates, and the influences on the properties of this alloy have been reported by other researchers; meanwhile, some innovative heat treatments have been developed [5-7]. Although the properties of 7055 alloys are clearly attractive, the processing of the alloy is difficult because of its high alloying element content [2-3, 8], the processing details of the alloy are unavailable in these literatures.

The fast development of computing techniques has contributed a lot to the wide application of finite element method (FEM) simulation in studying forming processes [9-10]. The flow stress relationship, which is used to describe the plastic flow properties, is necessary for the modeling of deformation. Numerical simulations can be truly reliable when a proper material flow stress relationship is built. The investigation of the hot compression deformation behavior of Al-7055 is necessary to perform the numerical simulation of forming and to establish the hot formation process parameters. As known, the microstructure during hot deformation is essential for analyzing the flow deformation of Al-7055; however, little attention has been given to the study on the microstructure during hot deformation.

The effects of deformation temperature and strain rate on the hot deformation characteristics of Al-7055 were examined by hot compression tests in the present work. Under different hot deformation conditions, the stress-stain flow curves were analyzed and the thermal-mechanical constitutive equation was established. The constitutive equations describing the dependence of the flow stress on strain, strain rate, and temperature were proposed and verified. Meanwhile, the microstructure was studied by transmission electron microscopy (TEM).

## 2. Experimental

The material used in the present work was commercial

Corresponding author: Liang-ming Yan E-mail: yanliangming@126.com

7055 aluminum alloy ingot. The composition is shown in Table 1. Axisymmetric compression (AC) specimens of ϕ10 mm×15 mm were machined from the homogenized material with grains of the major intercept length of 80±10 μm. The flat ends of the specimen were recessed to groove with a depth of 0.2 mm [11].

**Table 1. Composition of 7055 aluminum alloy wt%**

| Zn | Mg | Cu | Cr | Zr | Fe |
|---|---|---|---|---|---|
| 7.87 | 2.16 | 2.05 | <0.04 | 0.12 | 0.06 |
| Si | Mn | Ti | Ni | Al | |
| 0.04 | <0.05 | 0.019 | <0.05 | Bal. | |

Hot compression tests were conducted using a Gleeble-1500 thermal mechanical simulator at temperatures from 300°C to 450°C with a constant strain rate from $10^{-2}$ to 10 $s^{-1}$. The maximum of true strain is 0.7. In order to minimize the frictions between the specimens and the die during hot deformation, the grooves were filled with a lubricant of graphite mixed with machine oil. The variations of true stress and true strain were obtained from the controlling computer equipped with an automatic data acquisition system. The test specimens were compressed to certain strains, followed by immediate water quenching to room temperature to preserve the as hot-deformed microstructures. The specimens deformed under different conditions were sectioned longitudinally for microstructure observations. Thin foils for TEM investigation were prepared from 3-mm diameter discs punched out from 0.5-mm thick slices. The discs were ground and thinned by electropolishing using a solution mixture of 30vol% nitric acid in methanol as the electrolyte, maintained at –23°C and at a potential difference of 15 V. The foils were examined by H-800 TEM operating at 160 kV.

## 3. Results and discussion

### 3.1. True stress-strain curves and microstructure

Typical stress *vs.* strain curves obtained by compression tests are shown in Fig. 1. The curves are composed of work hardening stage, transition stage, and steady stage, which are characterized by an initial rapid increase in flow-stress to a broad peak due to the dominance of work hardening. When deformation exceeds the peak strain, softening caused by dynamic recovery overtakes hardening, followed by a very limited flow softening.

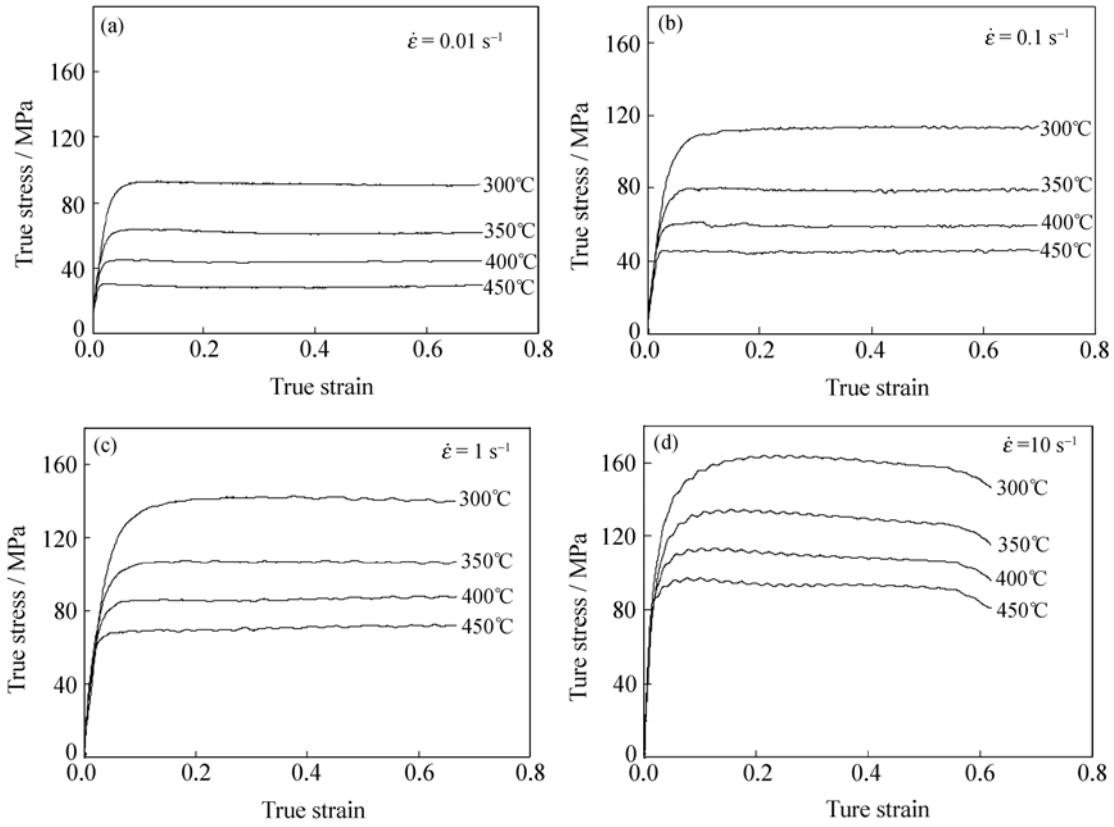


**Fig. 1. True stress-true strain curves of the alloy by hot compression at different strain rates: (a) $\dot{\varepsilon}$ =0.01 $s^{-1}$; (b) $\dot{\varepsilon}$ =0.1 $s^{-1}$; (c) $\dot{\varepsilon}$ =1 $s^{-1}$; (d) $\dot{\varepsilon}$ =10 $s^{-1}$.**

The microstructures of the as-deformed samples at the strain rate of 1 $s^{-1}$ and different temperatures are shown in Fig. 2. The dislocation tangle, and equiaxed cells with a diameter of 1 μm, and the dislocations pinned by second-phase particles are also observed (Fig. 2(a)). Some tangled cell walls become more regular dislocation networks or low angle grain boundaries. The cells transform to subgrains, and at this stage there is little change in the scale of the structure. It is characterized by the recovered grains containing a high density of sub-boundaries (Fig. 2(b)). Subgrains with dislocation walls within the grains (Fig. 2(b)) suggest that recovery is not completed or is continuous with the temperature increasing. The subgrains are equiaxed, roughly 1 to 2 μm in size, and the densities of dislocations in the subgrain interiors diminish (Fig. 2(c)). The recovery involves mainly a coarsening of the subgrain structure (Fig. 2(d)). The stored energy of a recovered substructure is still large, and can be further lowered by coarsening of the substructure, which leads to a reduction in the total area of the low angle boundary in the material.

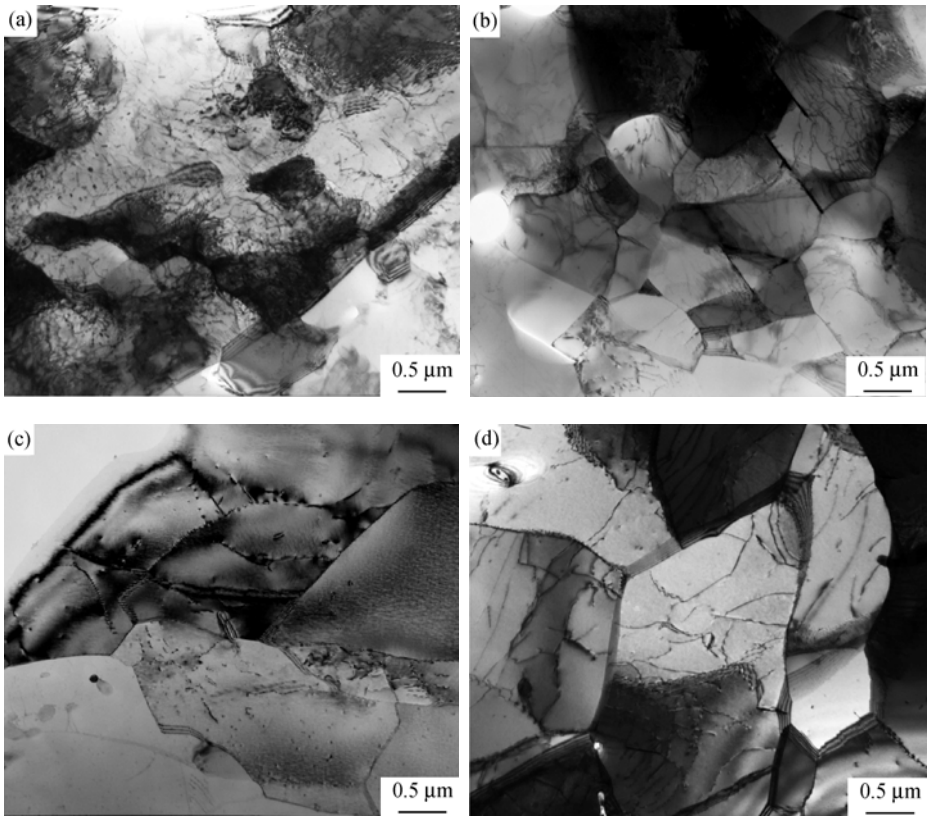


**Fig. 2. Microstructure of the 7055 aluminum alloy at different temperatures and the strain rate of 1 $s^{-1}$: (a) 300°C; (b) 350°C; (c) 400°C; (d) 450°C.**

Dynamic recovery is mainly affected by deformation temperature and processing time. The rate of cross slip which is the mechanism controlling the recovery rate is determined by the staking fault energy. For Al-7055, the rate of cross slip can be rapid due to the high stacking fault energy. During the dynamic recovery process, the stored energy of the material is lowered by the dislocation movement. There are two primary processes, *i.e.*, the annihilation of dislocations and the rearrangement of dislocations into lower energy configurations. Both processes are achieved by glide, climb, and cross-slip of dislocations [12]. Unequal numbers of dislocations of two signs are produced during deformation, and the excess cannot be removed by annihilation. These excess dislocations are arranged into lower energy configurations in the form of regular arrays or low angle grain boundaries (LAGBs). The driving force for subgrain growth arises from the energy stored in the subgrain boundaries.

At low temperatures and high strain rates, the dislocation generation (work hardening) factor is dominant, whereas at high temperatures and low strain rates, dynamic recovery dominates. Therefore, after hot deformation, the parameters of microstructure will be dependent on both strain and Zener-Hollomon parameter.

### 3.2. Effect of temperature and strain rate on the flow stress

The peak strain ($\varepsilon_p$) and peak stress ($\sigma_p$) obtained from the flow curves in Fig. 1 are listed in Table 2. Apparently, peak strain and peak stress progressively increase with the increase in strain rate when deformation temperature remains the same. The results indicate that 7055 aluminum alloy is sensitive to positive strain rate. Meanwhile, in the case of equal strain rate, the peak strain and peak stress gradually increase as the deformation temperature decreases.

**Table 2. Peak stress $\sigma_p$/MPa and peak strain $\varepsilon_p$ at different temperatures and strain rates**

| $\dot{\varepsilon}$ / $s^{-1}$ | $\sigma_p$ / MPa, $\varepsilon_p$ | | | |
|---|---|---|---|---|
| | 300ºC | 350ºC | 400ºC | 450ºC |
| 0.01 | 83.700, 0.076 | 57.380, 0.054 | 40.06, 0.031 | 27.47, 0.019 |
| 0.1 | 111.945, 0.133 | 80.030, 0.073 | 61.56, 0.043 | 46.08, 0.027 |
| 1 | 141.470, 0.156 | 107.035, 0.111 | 86.02, 0.070 | 69.53, 0.050 |
| 10 | 163.170, 0.192 | 133.310, 0.136 | 111.32, 0.091 | 94.06, 0.066 |

The variation of flow stress ($\sigma$) with deformation temperatures ($T$) and strain rates ($\dot{\varepsilon}$) can be clearly seen in Fig. 3. The flow stress at a true strain of 0.3 is plotted as a function of the deformation temperature and the logarithm of the strain rate in Figs. 3(a)-(b), respectively. For Al-7055, the flow stress increases when the deformation temperature decreases at the same strain rate, or the strain rate increases while the deformation temperature keeps unchanged. It is because low strain rates and high temperatures provide a longer time for energy accumulation and faster mobility of dislocations at boundaries for the dislocation annihilation and the formation and growth of subgrains.

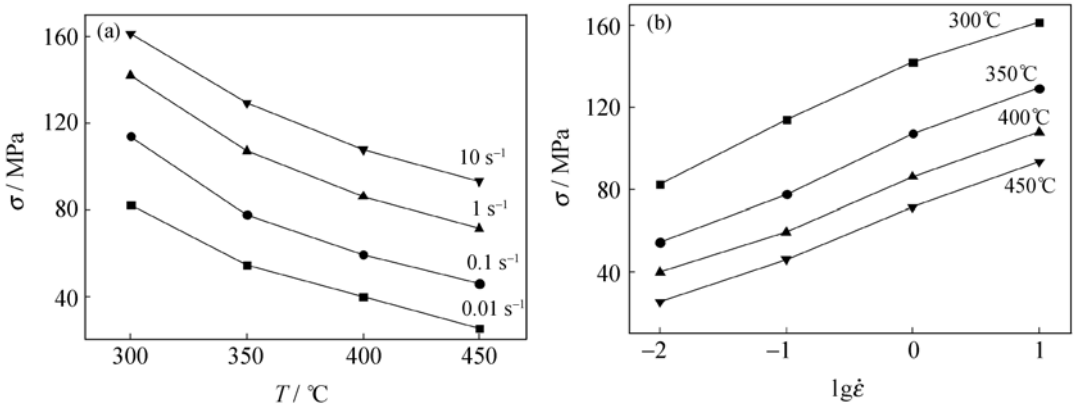


**Fig. 3. Influence of temperature and strain rate on the flow stress at the true strain of 0.3: (a) temperature; (b) strain rate.**

### 3.3. Establishment of hot deformation equation

The constitutive characteristics were detected more closely to investigate the plastic deformation behaviors of the 7055 aluminum alloy. The Zener-Hollomon parameter shown in the following equation can generally be used to characterize the combined effect of strain rate and temperature on the deformation process [13-14].

$$Z = \dot{\varepsilon}\exp\left(\frac{Q}{RT}\right) = A[\sinh(\alpha\sigma)]^n \tag{1}$$

where $Z$ is the Zener-Hollomom parameter representing the temperature-modified strain rate; $\dot{\varepsilon}$ the strain rate, $s^{-1}$; $R$ the universal gas constant, 8.31 $J{\cdot}mol^{-1}{\cdot}K^{-1}$; $T$ the absolute temperature, K; $Q$ the activation energy of hot deformation, $kJ{\cdot}mol^{-1}$; $A$ the structure factor, $s^{-1}$; $\alpha$ the temperature-independent material constant, $MPa^{-1}$; and $n$ the stress exponent.

It was reported that the activation energy can be calculated as [11]

$$Q = R\left[\frac{\partial \ln\dot{\varepsilon}}{\partial \ln[\sinh(\alpha\sigma)]}\right]_T\left[\frac{\partial \ln[\sinh(\alpha\sigma)]}{\partial(1/T)}\right]_{\dot{\varepsilon}} = Rn\left[\frac{\partial \ln[\sinh(\alpha\sigma)]}{\partial(1/T)}\right]_{\dot{\varepsilon}} \tag{2}$$

The slopes of $\ln(\dot{\varepsilon})$–$\ln[\sinh(\alpha\sigma)]$ at constant $T$ and $\ln[\sinh(\alpha\sigma)]$–$1000/T$ at constant strain rates were calculated as 5.7768 and 3.048, respectively, leading to a value of the action energy $Q$ of 146 kJ/mol. The value of $\alpha\sigma$ was calculated by means of an optimisation procedure, $\alpha$=0.01157

$MPa^{-1}$ gave the best correlation coefficient for the linear relationships between $\ln(\dot{\varepsilon})$–$\ln[\sinh(\alpha\sigma)]$ and $\ln[\sinh(\alpha\sigma)]$–$1000/T$.

The calculation of the Zener-Hollomon parameter $Z$ shows a good correlation for the compression data by considering $Q$=146 kJ/mol and $\alpha$=0.01157 $MPa^{-1}$, as shown in Fig. 4. The correlation coefficient is about 0.99. According to Eq. (1) and the regressed analysis results from Fig. 4, the value of $A$ can be computed as $5.62\times10^{11}$ $s^{-1}$.

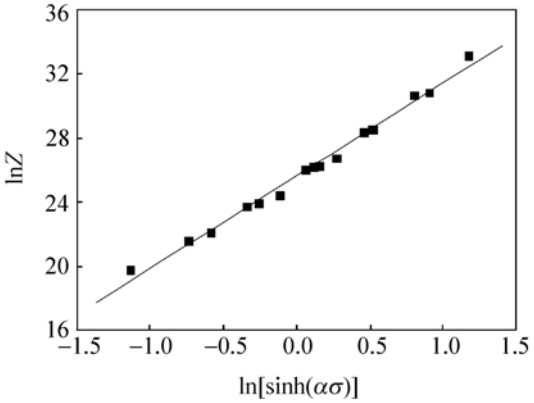


**Fig. 4. Relationship between flow stress and Zener-Hollomon parameter.**

Then, the flow stress ($\sigma$) can be written as a function of the Zener-Hollomon parameter, considering the definition of the hyperbolic law [15], as the following equation:

$$\sigma = (1/\alpha)\ln\left\{(Z/A)^{1/n} + [(Z/A)^{2/n} + 1]^{1/2}\right\} \tag{3}$$

According to the previous calculation, the Zener-Hollomon parameter for the 7055 aluminum alloy can be represented as

$$Z = \dot{\varepsilon}\exp(\frac{Q}{RT}) = A[\sinh(\alpha\sigma)]^n \tag{4}$$

Then, the flow stress constitutive equation of hot deformation for the 7055 aluminum alloy can also be expressed by the Zener-Hollomon parameter as

$$\sigma = 86.43\ln\left\{(Z/(5.62\times10^{11}))^{1/5.7768} + [(Z/(5.62\times10^{11}))^{2/5.7768} + 1]^{1/2}\right\} \tag{5}$$

### 3.4. Verification of the developed constitutive equations

In order to verify the developed constitutive equation of the 7055 aluminum alloy at elevated temperatures, the effects of strain on the flow stress are considered, the values of $Q$, $A$, $n$, and $\alpha$ can expressed as polynomial functions [16] as the following:

$$\begin{cases} Q = B_0 + B_1\varepsilon + B_2\varepsilon^2 + B_3\varepsilon^3 + B_4\varepsilon^4 + B_5\varepsilon^5 \\ n = D_0 + D_1\varepsilon + D_2\varepsilon^2 + D_3\varepsilon^3 + D_4\varepsilon^4 + D_5\varepsilon^5 \\ \ln A = E_0 + E_1\varepsilon + E_2\varepsilon^2 + E_3\varepsilon^3 + E_4\varepsilon^4 + E_5\varepsilon^5 \\ \alpha = F_0 + F_1\varepsilon + F_2\varepsilon^2 + F_3\varepsilon^3 + F_4\varepsilon^4 + F_5\varepsilon^5 \end{cases} \tag{6}$$

where $B_i$ are the coefficients of polynomial function $Q$; $D_i$ the coefficients of polynomial function $n$; $E_i$ the coefficients of polynomial function $\ln A$; $F_i$ the coefficients of polynomial function $\alpha$; $i$=0, 1,⋯, 5.

A series of constitutive Eq. (3) with different material constants $Q$, $A$, $n$, and $\alpha$ for different strain values from 0.08 to 0.5 are developed by the method to deduce the constitutive equation of peak stress. The coefficients of the polynomial functions are regressed in Table 3.

**Table 3. Coefficients of the polynomial functions of $Q$, $n$, $\ln A$, and $\alpha$**

| $Q$ | $n$ | $\ln A$ | $\alpha$ |
|---|---|---|---|
| $B_0$, 89.022 | $D_0$, 5.901 | $E_0$, 18.62361 | $F_0$, 0.01723 |
| $B_1$, 1519.666 | $D_1$, 1.757 | $E_1$, 266.79800 | $F_1$, –0.05535 |
| $B_2$, –15200.053 | $D_2$, –65.085 | $E_2$, –2844.98900 | $F_2$, 0.28581 |
| $B_3$, 67484.460 | $D_3$, 355.808 | $E_3$, 13348.69000 | $F_3$, –0.62068 |
| $B_4$, –134555.911 | $D_4$, –751.553 | $E_4$, –27578.81600 | $F_4$, 0.54654 |
| $B_5$, 98315.051 | $D_5$, 560.313 | $E_5$, 2057.98800 | $F_5$, –0.11158 |

Substituting the constants in Table 3 into Eqs. (1), (3), and (6), the flow stresses of the 7055 aluminum alloy at different deformation conditions can be obtained. Comparisons between the experimental and predicted flow stress curves at 300°C and 450°C are shown in Fig. 5. As can be observed from Fig. 5, agreement between the measured and calculated values is satisfied. In order to evaluate the accuracy of the developed constitutive equation, the error between the calculated flow stress ($\sigma_c$) and measured flow stress ($\sigma_m$) can be calculated as

$$\text{error} = \frac{\sigma_c - \sigma_m}{\sigma_m}\times100\% \tag{7}$$

Using this calculation, the results of this evaluation for

flow stress are calculated at strains within the range of 0.08-0.5 and the maximum interval of 0.1 under strain rate from 0.01 to 1 $s^{-1}$. It can be found that the error in the flow stress estimate is less than 5%. Moreover, the mean differences between the calculated and measured flow stress under different conditions of 0.01 $s^{-1}$ (300°C), 1 $s^{-1}$ (300°C), 0.01 $s^{-1}$ (450°C), and 1 $s^{-1}$ (450°C) are –0.81%, 0.44%, –0.25%, and 0.92%, respectively. Similar results can be observed under other conditions, which indicate that the proposed model can properly estimate the flow stress of 7055 aluminum alloy. Therefore, the proposed model can be used to numerically analyze the hot forming processes.

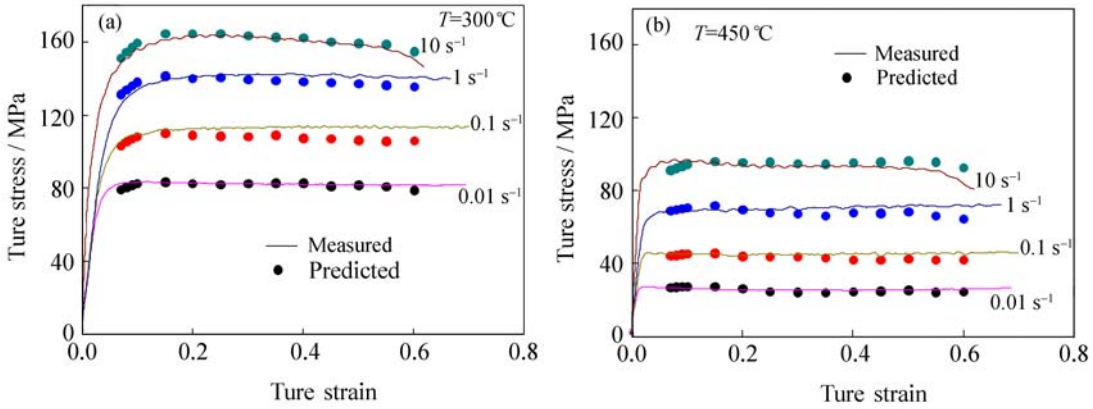


**Fig. 5. Comparison between the predicted and measured flow stress curves at 300°C (a) and 450°C (b).**

## 4. Conclusion

The deformation characteristics of the commercial 7055 aluminum alloy were investigated by means of the hot compression test over a practical range of temperatures and strain rates. The microstructures of as-deformed 7055 alloy are observed, which indicate that dynamic recovery is the main softening mechanism. The flow stress of 7055 aluminum alloy rises with the increase of strain rate and the decrease of deformation temperature, which can be represented by a Zener-Hollomon parameter in an exponent-type equation. The strain hardening coefficient $n$ and deformation activation energy $Q$ are evaluated by linear regression analysis, and the flow stress constitutive equations of 7055 aluminum alloy during hot compression are developed. Comparisons between the predicted and measured results show that the error in the flow stress estimate is less than 5%. Moreover, comparisons between the predicted results and the measured results indicate that the proposed constitutive equations can be used for analyzing the flow stress of the Al 7055 aluminum alloy forming processes.

## References

[1] R. Kaibyshev, T. Sakai, F. Musin, *et al.*, Superplastic behavior of a 7055 aluminum alloy, *Scripta Mater.*, 45(2001), No.12, p.1373.

[2] C. Mondal, A.K. Mukhopadhyay, T. Raghu, and V.K. Varma, Tensile properties of peak aged 7055 aluminum alloy extrusions, *Mater. Sci. Eng. A*, 455(2007), No.3, p.673.

[3] J.Z. Chen, L. Zhen, W.Z. Shao, *et al.*, Through-thickness texture gradient in AA 7055 aluminum alloy, *Mater. Lett.*, 62(2008), No.1, p.88.

[4] M. Dixit, R.S. Mishra, and K.K. Sankaran, Structure-property correlations in Al 7050 and Al 7055 high-strength aluminum alloys, *Mater. Sci. Eng. A*, 478(2008), No.1-2, p.163.

[5] S.D. Liu, X.M. Zhang, M.A. Chen, *et al.*, Influence of aging on quench sensitivity effect of 7055 aluminum alloy, *Mater. Charact.*, 59(2008), No.1, p.53.

[6] Z.H. Li, B.Q. Xiong, Y.A. Zhang, *et al.*, Ageing behavior of an Al-Zn-Mg-Cu alloy pre-stretched thick plate, *J. Univ. Sci. Technol. Beijing*, 14(2007), No.3, p.246.

[7] K.H. Chen, H.W. Liu, Z. Zhang, *et al.*, The improvement of constituent dissolution and mechanical properties of 7055 aluminum alloy by stepped heat treatments, *J. Mater. Process. Technol.*, 142(2003), No.1, p.190.

[8] I. Nikulin, R. Kaibyshev, and T. Sakai, Superplasticity in a 7055 aluminum alloy processed by ECAE and subsequent isothermal rolling, *Mater. Sci. Eng. A*, 407(2005), No.1-2, p.62.

[9] Q. Zhu, M.F. Abbod, J.T. Alamantes-Silva, *et al.*, Hybrid modelling of aluminium magnesium alloys during thermomechanical processing in terms of physically-based, neuro-fuzzy and finite element models, *Acta Mater.*, 51(2003), No.17, p.5051.

[10] Q.J. Chen, Y.L. Kang, H. Yu, *et al.*, Research on microstructural evolution and dynamic recrystallization behavior of JB800 bainitic steel by FEM, *J. Univ. Sci. Technol. Beijing*, 15(2008), No.3, p.250.

[11] J. Shen, *Study on the Plastic Deformation Behavior of 2091 Al-Li Alloy at Elevated Temperatures* [Dissertation] (in Chinese), Central South University of Technology, Changsha, 1996, p.22.

[12] F.J. Humphreys and M. Hatherly, *Re-crystallization and Re-*

*lated Annealing Phenomena*, Pergamon Press, Oxford, 2004, p.416.

[13] J.T. Liu, G.Q. Liu, B.F. Hu, *et al.*, Hot deformation behavior of FGH96 superalloys, *J. Univ. Sci. Technol. Beijing*, 13(2006), No.4, p.319.

[14] H. Shi, A.J. McLaren, C.M. Sellars, *et al.*, Constitutive equations for high temperature flow stress of aluminum alloys, *Mater. Sci. Technol. A*, 13(1997), No.3, p.210.

[15] X.H. He, Z.Q. Yu, G.M. Liu, *et al.*, Mathematical modeling for high temperature flow behavior of as-cast Ti-45Al-8.5Nb-(W,B,Y) alloy, *Mater. Des.*, 30(2009), No.1, p.166.

[16] M. Mulyadi, M.A. Rist, L. Edwards, and J.W. Brooks, Parameter optimisation in constitutive equations for hot forging, *J. Mater. Process. Technol.*, 177(2006), No.1-3, p.311.